

Chapter 3

Obstacle induced phase separation of micro swimmers

Abbreviations/Acronyms: **ABPs** (active Brownian particles), **MIPS** (motility induced phase separation), ***Pe*** (Peclet number), **PDF**(probability distribution function), **SPPs** (self-propelled particles).

3.1 Introduction

In the previous Chapter.2, We have modeled a binary mixture of active and passive Brownian particles and observed the steady state properties and growth kinetic of passive particles in the presence of active Brownian particles (ABPs). In this chapter we address the influence of an obstacle on the properties of ABPs. As we have discussed earlier, the study of active matter spans a vast range of far from equilibrium systems where energy input takes place at each constituent level and the consumed energy is transduced by the constituents into mechanical work [Marchetti et al. \(2013\)](#); [Ramaswamy \(2010\)](#). These systems range from micro scale [Berg \(2004\)](#); [Rappel et al. \(1999\)](#) to macro scale [Ballerini et al. \(2008b\)](#); [Vicsek et al. \(1995\)](#), evince number of novel phenomena like collective coherent motion

Couzin et al. (2005); Kudrolli et al. (2008b); Sokolov et al. (2007); Vicsek (2001), phase separation Fily & Marchetti (2012), pattern formation Gopinath et al. (2012) and so on. These features exhibited by active systems make it a fascinating class of problem to work on and have drawn attention of researchers in past decades. Active Brownian particle is an example of self-propelled particle, which has a preferred direction of motion, constitutes a theoretically idealized model for active systems. The number of recent works on ABPs show the existence of motility induced phase separation (MIPS) Fily & Marchetti (2012); Fily et al. (2014); Speck et al. (2014) Buttinoni et al. (2013b); Cates & Tailleur (2015b); Palacci et al. (2013); Solon et al. (2018); Tailleur & Cates (2008), a phenomena in which self propelled particles interacting via short range repulsion, tend to phase separate into dense cluster and dilute gas like phase. The phenomena of MIPS, implies the self blocking of the particles that arises due to the interplay between the directed motion and exclusion of particles from occupying the same space. This leads to the increment in local density of active particles and subsequently there is sufficient decay in their self propulsion speed Bickmann & Wittkowski (2020); Cates & Tailleur (2013); Tailleur & Cates (2008), gives arise the self blocking and so MIPS. In the studies Wysocki et al. (2014); Zöttl & Stark (2014), it is found that phenomena of MIPS is subject to packing densities of active particles and their self-propulsion speed. Various studies on ABPs have observed that the particles tend to phase separate for packing density above than the critical value 0.4 Fily & Marchetti (2012) and Peclet number (Pe) (analogous to their self propulsion speed) greater than 50 (Redner et al., 2013a).

Apart from the studies on the clean system of active particles, presence of disorder in the background medium that creates a heterogeneous environment for the system of active particles, has become an appealing area of research Bechinger et al. (2016); Pinçe et al. (2016). Study on active run and tumble particle on disordered landscape composed of fixed

obstacles has shown the active matter transport and jamming as depending on the density of the obstacles [Reichhardt & Reichhardt \(2014\)](#). Many numerical and experimental studies are performed on the dynamics of self propelled particles in a crowded environment [Chepizhko & Peruani \(2013\)](#); [Morin et al. \(2017\)](#); [Peruani & Aranson \(2018\)](#); [Reichhardt & Reichhardt \(2018\)](#); [Sándor et al. \(2017\)](#). The above works have mainly focused on the dynamics of active particles and observed it as a function of obstacle density. In our study, we focus on observing the influence of a single quenched obstacle on the steady state properties of a system of ABPs. We tune the size of the obstacle, packing density of the ABPs and Peclet number. We observe that obstacle has a significant effect on the properties of ABPs.

We construct a minimal model of small ABPs in the presence of a random quenched obstacle on a two-dimensional substrate interacting through a short-range soft-repulsive interaction. The self-propulsion force and soft-repulsive interaction are the driving force for the dynamics of active particles and obstacle is fixed in space and time. The dynamics and steady state of ABPs are observed by tuning the size of the obstacle, Peclet number and packing density of the ABPs. We observe the phase separation of ABPs in the presence of obstacle and compare it with the system of ABPs without obstacle. It is observed that the obstacle induces the phase separation at much lower packing density for the same Peclet number, where the system of ABPs without obstacle is non phase separated. We plot the phase diagram in the plane of Peclet number and packing fraction for various sizes of the obstacle and find a shift in the phase boundary towards the lower value of packing fraction and Peclet number. We also find that phase separation very much depends on the size ratio of the obstacle vs. ABPs. Finally we conclude that obstacle enhances the phase separation in the collection of ABPs.

We discuss our study into the following manner. In next section 3.2, we describe the model in detail. Section 3.3 discusses our findings and finally in section 3.4 we conclude our results.

3.2 Model

We consider a system of ABPs and an obstacle on a two-dimensional substrate. The obstacle is quenched in space and time. The active particles and obstacle are modeled as discs of radius r_a and r_o respectively, where $r_o > r_a$, obstacle is larger in size compare to active particles. The size ratio $S = \frac{r_o}{r_a}$ is one of the crucial parameters in the model. The radius of the active particles is kept fixed and radius of obstacle is tuned to vary the size ratio. The another control parameter in our system is, packing fraction of the ABPs, which is defined as $\phi_a = \frac{\pi r_a^2 N}{L^2}$ where N is the number of ABPs in the system. The ABPs are defined by their position $\mathbf{r}_i(t)$ and their orientation $\theta_i(t)$, which determines their direction of self-propulsion. They self-propel along their direction of orientation $\theta_i(t)$ with a constant self-propulsion speed v_0 .

The governing overdamped Langevin's equations of motion for position and orientation updates of the i^{th} active particle are

$$\frac{d\mathbf{r}_i^a(t)}{dt} = v_0 \hat{\mathbf{n}}_i(t) + \mu \sum_{j \neq i} \mathbf{F}_{ij}(t) \quad (3.1)$$

where $\hat{\mathbf{n}}_i(t) = (\cos(\theta_i(t)), \sin(\theta_i(t)))$ is the unit direction of self-propulsion of the ABP.

The change in the orientation of the active particle is given by:

$$\frac{d\theta_i}{dt} = \sqrt{v_r} \eta_i(t) \quad (3.2)$$

here $\eta_i(t)$ is the random Gaussian white noise with mean zero and variance, $\langle \eta_i^r(t)\eta_j^r(t') \rangle = \delta_{ij}\delta(t-t')$, and v_r is the rotational diffusion constant of active particles. $\mathbf{F}_i(t)$ is the force acting on the i^{th} particles, due to all other particles interacting with it

$$\mathbf{F}_i(t) = \sum_{j \neq i} \mathbf{F}_{ij}(t) \quad (3.3)$$

The force is obtained from the soft-repulsive pair potential $\mathbf{F}_{ij} = -\nabla U(r_{ij})$, where

$U(r_{ij}) = K(r_{ij} - (r_{\alpha i} + r_{\alpha' j}))^2$ if $r_{ij} \leq (r_{\alpha i} + r_{\alpha' j})$ and 0 otherwise. $r_{ij} = |r_i - r_j|$ and K is the force constant and r_{α} , is the radius of active particles or obstacle for α and $\alpha' = a$ or o respectively. v_r^{-1} is the time scale over which the orientation of an active particle changes. Hence, $l_p = v_0 v_r^{-1}$, is the persistence length or run length, is the typical distance travelled by an active particle before it changes its direction. In our study, $l_p = 30r_a$ to $150r_a$ is tuned by tuning SPPs v_0 . We define the Peclet number, $Pe = \frac{l_p}{r_a}$ as the ratio of persistent length to the size of active particles. The packing fraction ϕ_a , size ratio S and Peclet number Pe are the three tuning parameters in the model.

We start with random non-overlapping arrangement of active and passive particles on a two dimensional square substrate of linear dimension $L = 320r_a$ with periodic boundary condition in both the directions. The equations 3.1 – 3.2, are updated and one simulation step is counted after updation of all the particles once. The time step $\tau = 10^{-5}v_r^{-1}$, where $v_r^{-1} = 10^2$ and total 8×10^4 simulation steps are used to get the results. All the lengths and times are measured in terms of r_a and v_r^{-1} . We have used 20 independent realisations to get averaged data and different realisations are obtained by initialising the system with the similar initial conditions but different configurations. We characterise the effect of different parameters on the steady state of the athermal active particles in the presence of random quenched obstacle.

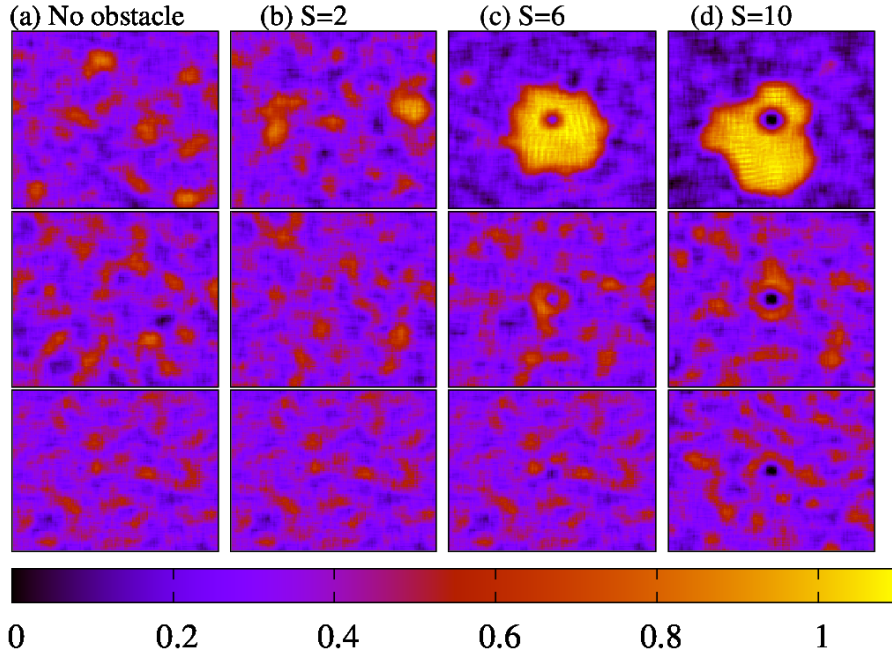


Fig. 3.1 (color online) Time evolution of the coarse grained local density, ϕ_{loc} of ABPs is shown for $\phi_a = 0.35$ for system with no obstacle, and obstacle with size ratio $S = 2, 6$ and 10 from left (a) – (d) at fixed $Pe = 100$. The snapshots from bottom to top panel is in increasing time direction for times $10^{-2}v_r^{-1}$, $10^{-1}v_r^{-1}$ and v_r^{-1} respectively. Color bar shows the local density in area of $12r_a \times 12r_a$.

3.3 Results

3.3.1 Phase Separation

We first discuss the time evolution of the system. We measure the local density, ϕ_{loc} of self-propelled particles in a coarse-grained region of size $12r_a \times 12r_a$. We observe that as the system evolves, particles start to accumulate around the obstacle and particle rich region grows with time. The particles show the consistent behavior and undergo non equilibrium clustering for very low packing fraction $\phi_a = 0.35$ and Peclet number $Pe = 30$. We further confirm our result, for different sizes of the obstacle and Peclet number of the self propelled particles. We find that the size of the obstacle and Peclet number play a major role in the formation of cluster. The large size of the obstacle and high Peclet number promotes the phase separation in active particles. For $\phi = 0.35$, time evolution of the

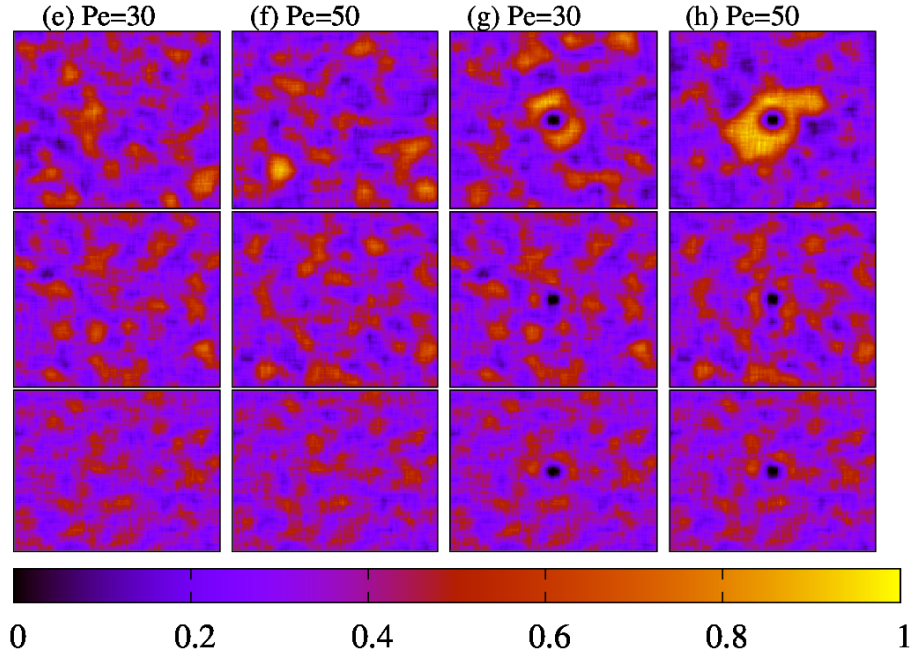


Fig. 3.2 (color online) Time evolution of the coarse grained local density of ABPs is shown for $\phi_a = 0.35$ for system with no obstacle e and f , and obstacle of size ratio 10, g and h for $Pe = 30$ and 50 respectively. The snapshots from bottom to top panel is for times $10^{-2}v_r^{-1}$, $10^{-1}v_r^{-1}$ and v_r^{-1} respectively. Color bar shows the local density in area of $12r_a \times 12r_a$.

system is shown in fig 3.1 and fig 3.2. 3.1 corresponds to fixed Peclet number $Pe = 100$ and varying the size of the obstacle and fig 3.2 is for fixed size ratio $S = 10$ and tuned Peclet number and both are compared with the case when no such obstacle is present in the system.

Next we quantify the phase separation by observing the probability distribution function (PDF) of local density, $P(\phi_{loc})$ of ABPs in for different parameters. We observe it for three different packing fractions $\phi_a = 0.3, 0.35$ and 0.4 at fixed size ratio, $S = 10$ and for different Peclet number Pe . We keep the packing density ≤ 0.4 because in general clean system of ABPs shows the MIPS for packing density ≥ 0.4 . We compare it with the system of ABPs when no such obstacle is present in the system.

Fig 3.3 shows the local density distributions for three different ϕ and for both the cases, with and without obstacle. The single peak shows the density distributions for the system with no phase separation and as the phase separation occurs it becomes bimodal.

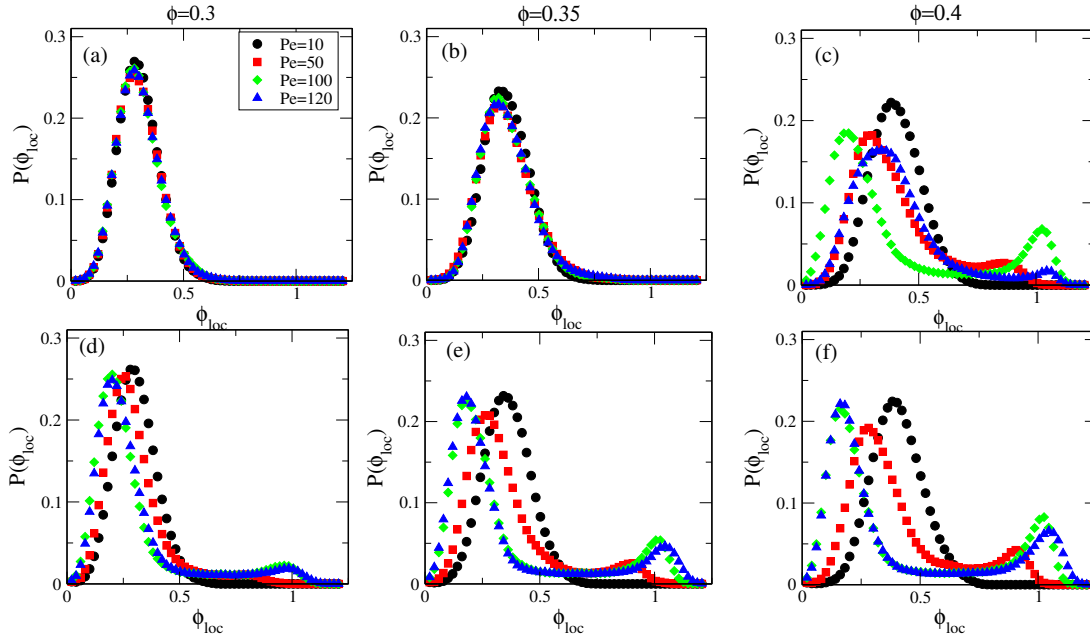


Fig. 3.3 (color online) The probability distribution function (*PDF*) of local density $P(\phi_{loc})$, are shown for three packing fractions $\phi_a = 0.3, 0.35$ and 0.4 as a function of size ratio, S and Peclet number, Pe . (a) – (c) are for the system with no obstacle and (d) – (f) are when there is obstacle present in the system.

Interestingly, we find that the $P(\phi_{loc})$ shows a small peak at high density region, $\phi_{loc} \sim 1$ for very small $\phi_a \sim 0.3$ for large size ratio which is not present in the case of system of ABPs without obstacle. For $\phi = 0.35$, the second peak becomes more pronounced and it shows the coexistence of dilute gas and dense cluster like phase. The peak for the low value of ϕ_{loc} correspond to the randomly moving particles (low density region, gas like phase) and the peak at high value of $\phi_{loc} \sim 1$ shows the particles, which are the form of the cluster (high density region, liquid like phase). Hence the system coexist with the gas and liquid like phase for large S , even at very small packing fraction of ABPs. Thus the system develops a binodal envelop, which is the plot of location of two peaks and shown in fig 3.4. This shows the range of parameters for which the phase separated densities collapse onto a single coexistence curve.

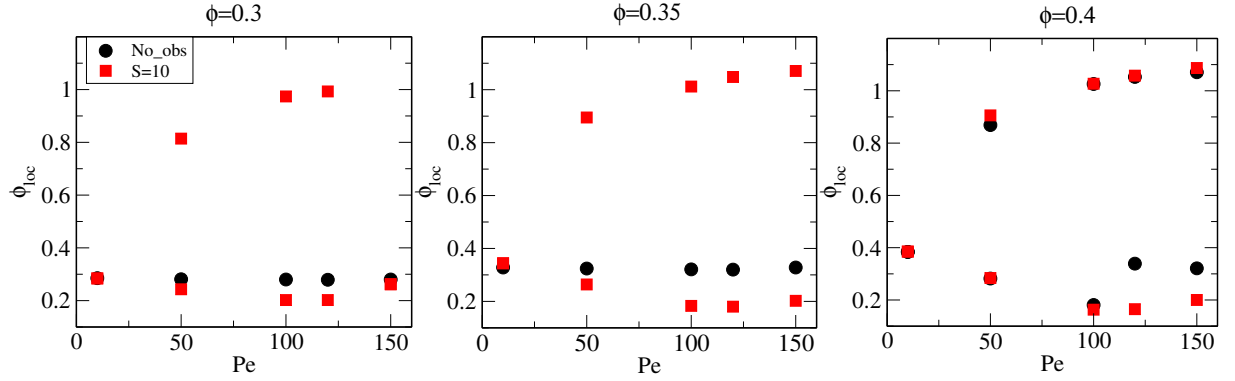


Fig. 3.4 (color online) shows the phase coexistence curves for three $\phi_a = 0.3, 0.35$ and 0.4 for system with no obstacle (black \circ) and for system with obstacle of size 10 times larger than ABP (red \square). The number on Y-axis shows the location of peaks of *PDF* of ϕ_{loc} . X-axis is the Peclet number.

3.3.2 Steady state phase diagram

Further we draw the phase diagram by measuring the $P(\phi_{loc})$ and finding the difference in location of low and high density peaks, which is calculated from the PDF of the local densities. For the value of the difference in low and high density peaks less than 0.5, the system is in homogeneous state and when the difference is greater than 0.5, the system is in phase separated state. The mean value, 0.5 corresponds to the phase boundary of the system. We plot the phase diagram in fig 3.5 for two different size ratios in the plane of Pe and ϕ_a and compare it with the system of ABPs without obstacle. We find that the phase boundary of the system with coexistence phase and pure gas like phase shifts towards lower Peclet number and packing fraction values in presence of obstacle and the shift in boundary is a function of the size of the obstacle. In fig 3.6 and 3.7 we show the real space steady state snapshots of the ABPs for the case without obstacle and in presence of random quenched obstacle for $S = 10$ respectively in plane of Pe and ϕ_a . The snapshots show the clear significance of presence of obstacle in the system of ABPs and verifies the shift in phase boundary as shown in fig 3.5.

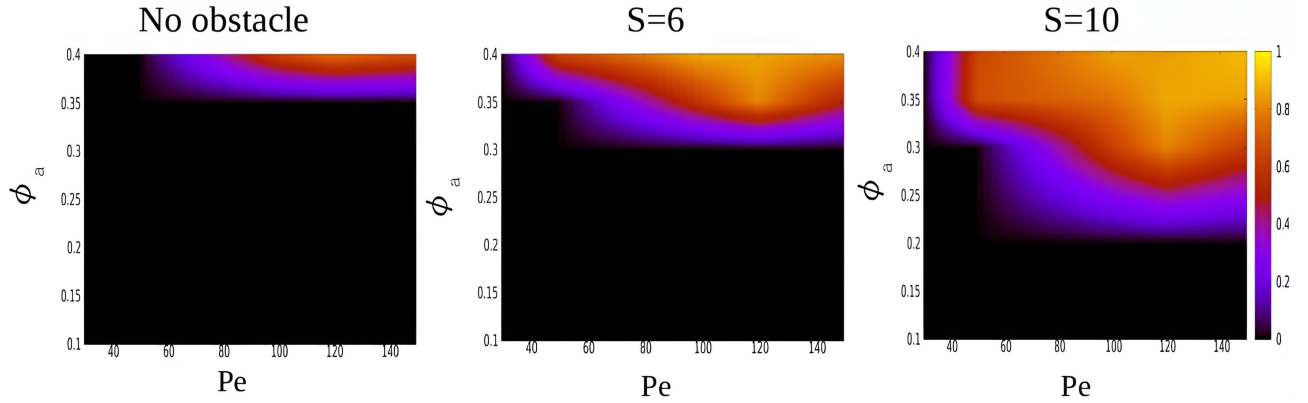


Fig. 3.5 (color online) shows the phase diagram in the plane of ϕ_a and Pe for the system with no obstacle and with obstacle of size 6 and 10 times larger than ABP. The range of ϕ_a varies from 0.1 to 0.4 and for Peclet number it goes from 30 to 150. Color bar shows the values of the differences in location of low and high density peaks.

3.4 Conclusion

We have studied the phase separation and steady state properties of ABPs in presence of single quenched obstacle and compare the results with the case when there is no obstacle present in the system. We have modeled the system on a two dimensional substrate with periodic boundary conditions. The particles are interacting through soft repulsive interaction. We find that in the presence of obstacle, the ABPs tend to phase separate at packing fraction, $\phi \sim 0.35$, lower than the observed value of critical packing, $\phi > 0.4$ for a clean system of ABPs for the phase separation. Hence obstacle enhances the clustering in the system. Further we observe the *PDF*, $P(\phi_{loc})$ of ϕ_{loc} and find that the system shows bimodal peaks corresponding to the coexistence of low density and high density regions. Next we observe the phase diagram in the plane of Peclet number and size ratio and find that the phase boundary shifts as we go towards large size of the obstacle. Our study provides the understanding of influence of a heterogeneous environment on the properties of ABPs.

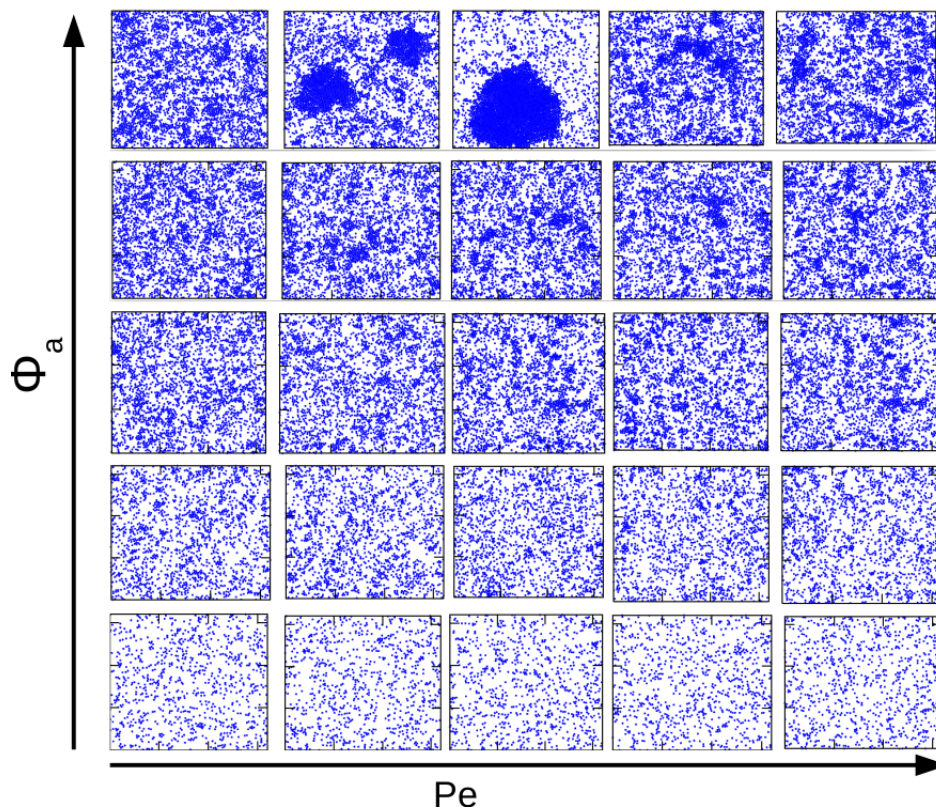


Fig. 3.6 (color online) Real space snapshots of clean system of ABPs in steady state in plane of ϕ_a and Pe . Pe varies from 30 – 150 (left to right) and ϕ_a goes from 0.1 – 0.4 (bottom to top).

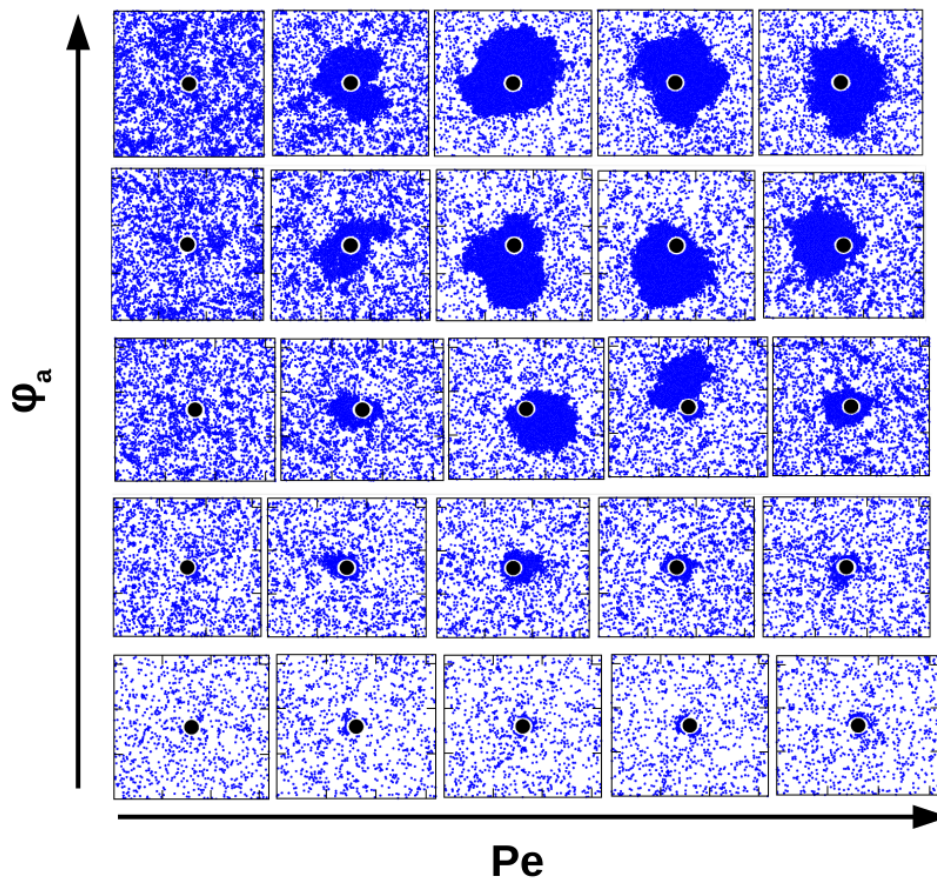


Fig. 3.7 (color online) Real space snapshots of the system of ABPs in presence of single quenched obstacle in steady state in plane of ϕ_a and Pe . Pe varies from 30 – 150 (left to right) and ϕ_a goes from 0.1 – 0.4 (bottom to top)